

Mechatronics Design and Robotic Simulation of Serial Manipulators to Perform Automation Tasks in the Avocado Industry

Carlos Paredes¹, Ricardo Palomares², Josmell Alva³, José Cornejo⁴

Department of Mechatronic Engineering, Universidad Nacional de Trujillo, Trujillo, Peru^{1, 2, 3}
Universidad Tecnológica del Perú, Lima, Peru⁴

Abstract—Peru is considered one of the principal agroindustrial avocado exporters worldwide. At the beginning of 2022, the volume exported was 8.3% higher than in 2021, so the design and simulation of a pick and place and palletizing cell for agro-exporting companies in the Region of La Libertad was proposed. A methodology was followed that presented a flow diagram of the design of the cell, considering the size of the avocado and the dimensions of the box-type packaging. The forward and inverse kinematics for the Scara T6 and UR10 robots were developed in Matlab according to the Denavit-Hartenberg algorithm, and 3D CAD, dynamic modeling, and trajectory calculation were performed in Solidworks using a "planner" algorithm developed in Matlab, which takes into account the start and end points, maximum speeds, and travel time of each robot. Then, in CoppeliaSim, the working environment of the cell and the robots with their respective configurations are created. Finally, the simulation of trajectories is performed, describing the expected movement, getting the time of the finished task was calculated, where the Scara T6 robot had a working time of 1.18 s and the UR10 of 2.32 s. For 2023 - 2025, its implementation is proposed in the Camposol Company located in the district of Chao - La Libertad, considering the dynamic control of the system.

Keywords—*Mechatronic design; inverse kinematics; dynamic modeling; pick and place; palletizing; Scara robot; universal robot; robot manipulators; path tracking simulation; kinematic control*

I. INTRODUCTION

In 2022, Peru's non-traditional exports grew up by 19.4% compared to 2021, with the agricultural sector accounting for 43.7% of this growth, with avocado as the main product, with a value of 528,727 tons of exported volume [1], [2]. Camposol is considered as the largest Peruvian agro-exporting company, with USD 112,645,000 in shipments [3]. Since 2018 the company developed a strategic expansion plan and purchased 1000 ha in Uruguay [4]. In 2020, Camposol's CEO prioritized the avocado packing process [5]. Various improvement proposals for the packaging process are being studied worldwide. A notable initiative is the development of a 4-degree-of-freedom fruit sorting robot, based on the evaluation of both fruit size and color, using advanced digital image processing techniques. The results have been promising, achieving sorting times of 11.91 seconds for red tomatoes and 11.76 seconds for green ones. Furthermore, it is highlighted that the variation in sorting times is linked to the arrangement of the boxes within the environment. This variability becomes

significant when considering scenarios similar to avocado packing [6]. In another investigation, a control system for a palletizing robot is designed using RobotStudio. This study has demonstrated optimal performance in palletizing tasks using precise input/output (I/O) control logic, which ensures high stability, safety, and efficiency within the simulation environment. This work leads to the proposal to create a virtual environment that simulates real-world conditions for the avocado packing process, elevating it to a TRL5 level [7]. The derivation of the direct and inverse kinematics of the ABB IBR 140 robot was proposed using Denavit-Hartenberg and (DH) analysis and analytical geometric approximations, respectively. The transformation matrices were validated in Matlab and subsequently simulated in RobotStudio to verify their accuracy [8]. A methodology based on the Digital Twin (DT) concept for flexible pick-and-place robotic work cells was also designed to facilitate the development process by providing guidance. This proposal leads to the creation of a design approach for a robotic work cell based on the application of pick-and-place avocado picking and placing for subsequent simulation [9]. A packaging algorithm called Jampack was developed, which has a Failure Recovery Module (FRM) for a robotic manipulator, allowing the system to reach a faster completion of the system [10]. Another algorithm implemented is ResNet-18 for real-time Hass avocado grading, which seeks to achieve non-invasive grading to reduce damage caused by handling. After several processing steps, the image acquisition system achieved an accuracy of 98.72%, a specificity of 98.52%, and a score of 98.08% [11]. However, human-machine collaboration for these applications is still relevant and a topic of ongoing research. This has led to another study aimed at evaluating the avocado harvesting process. After carrying out 41 different tests, a significant increase in yield, measured in the loading zone, from 15% to 80% was found. Also, total harvested production has increased from 23% to 85%, with a minimal increase in human labor load from 1% to only 16% [12]. On the other hand, a soft humanoid hand designed to firmly grip a wide variety of objects, regardless of their morphology, is presented. On this hand, the fingers are constructed with flexible hybrid pneumatic actuators (FHPA). Using a theoretical evaluation model, a balance between the required flexibility and stiffness has been achieved. This innovation offers fast responsiveness and significant gripping force, suitable for fruit picking, product packaging, and handling of fragile objects [13].

This project contributes to Sustainable Development Goals 8 and 9 set by the United Nations, as they focus on achieving higher economic productivity through the utilization of technology and innovation, as well as increasing scientific research and improving technological capacity in industrial sectors, particularly in developing countries, by 2030 [14].

Therefore, the increase in demand for avocado exports poses a challenge if the packaging process is not accelerated, since currently, both at Camposol and other companies, the picking and placing of avocados is performed by workers, resulting in delays in procedures and order deliveries. For this reason, it is proposed to design and simulate a pick and place and palletizing cell, where two robots will perform the process automatically.

The structure of this paper is divided as follows: Section I contains the introduction, which details both the problem and its solution. Section II covers the materials and methods, where the design is based on a methodology that includes kinematic and dynamic analysis, trajectory tracking calculations, and real-time simulation. Section III presents the results derived from the simulation of the robotic cell. Finally, Section IV consolidates the conclusions and future work of the project.

II. MATERIALS AND METHODS

The proposed methodology for designing and simulating the avocado pick and place and palletizing cell, using Matlab and CoppeliaSim, is shown in Fig. 1.

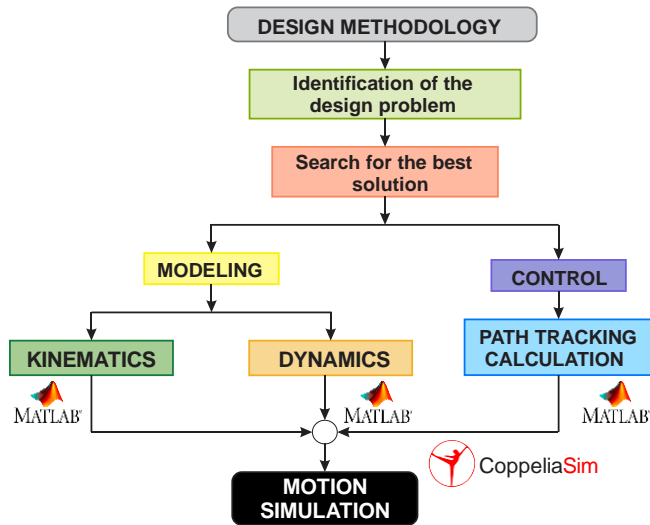


Fig. 1. Flow chart for the design of an avocado pick and place and palletizing cell.

The cell design consists of two tasks that are performed sequentially. The first one is performed by an Epson Scara T6 robot, which picks and places the Hass avocado in a cardboard box (pick and place), using a vacuum suction cup as the final effector, considering the caliber (weight) of the Hass avocado, which varies according to the country to be exported [15], as shown in Table I.

On the other hand, there is a Universal Robots UR10 robot, which picks up the boxes and groups them in rows and columns (palletizing), using a four vacuum suction cup holder

as an end effector, considering the shape, weight, and distribution of the boxes [16], as shown in Table II.

TABLE I. HASS AVOCADO EXPORT CALIBER

Avocado	Avocado Caliber Requirements by Country				Fruit Weight (g)
	USA	Japan	Canada	European Union	
Hass	32	–	12	12	300 – to more
	36	18	14	14	300 – 330
	40	20	16	16	265 – 300
	48	24	18	18	205 – 265
	60	30	20	20	170 – 205
	70	–	22	22	150 – 170
	84	–	24	24	120 – 150

TABLE II. BOX FEATURES

Type of Box	Recommended Avocado Packaging Features		
	Dimensions (mm)	Average Weigh (kg)	Pallet
Cardboard	440 x 338 x 186	11	88 - 96
	406 x 254 x 97	4	228 - 264
Plastic	300 x 500 x 150	10	120

A. Forward and Inverse Kinematic Model

The Scara T6 and UR10 robots are 3 DOF (two rotational and one linear) and 6 DOF (rotational only), respectively [17], [18]. Moreover, their Cartesian reference systems and the motion of each joint are shown in Fig. 2 and Fig. 3 [19].

Eq. (1) presents the T_n^0 homogeneous transformation matrix, which expresses the position and orientation of each robot [20] and [21]. Eq. (2) and (3) represent the basic T_3^0 and T_6^0 transformations, where n is the number of joints.

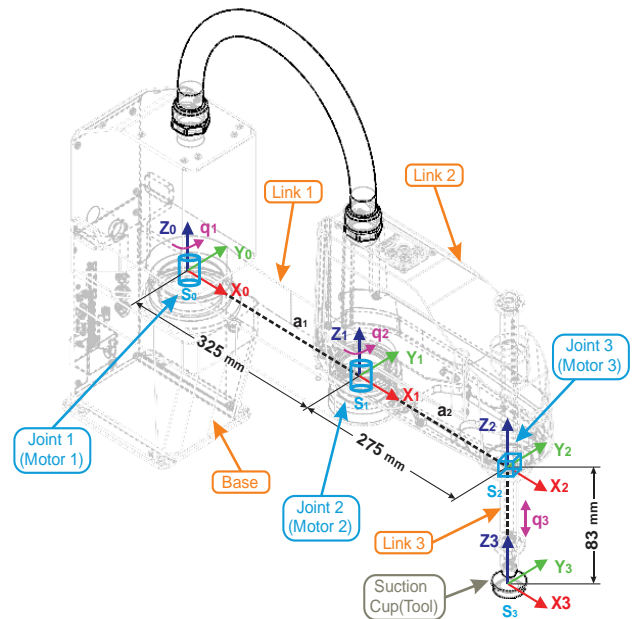


Fig. 2. Cartesian reference system and lengths for the Scara T6 robot.

$$\square T_n^0 = \begin{bmatrix} n_{nx1} & o_{nx1} & a_{nx1} & P_{nx1} \\ 0 & 0 & 0 & 1 \end{bmatrix} \quad (1)$$

$$T_3^0 = A_1^0 A_2^1 A_3^2 \quad (2)$$

$$T_6^0 = A_1^0 A_2^1 A_3^2 A_4^3 A_5^4 A_6^5 \quad (3)$$

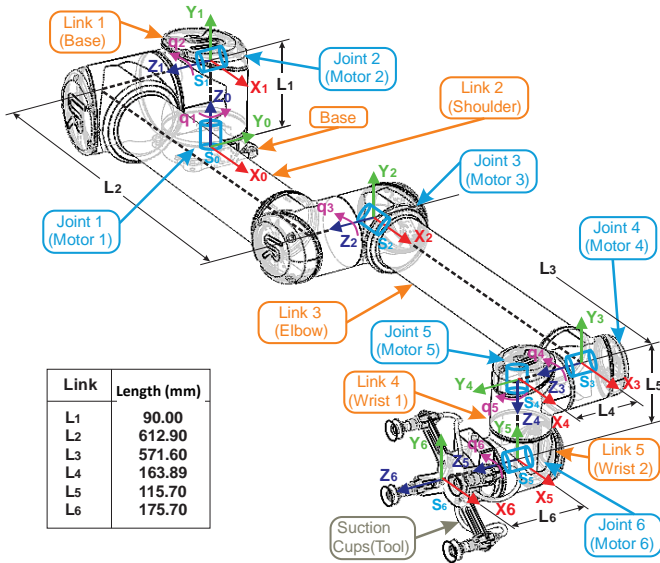


Fig. 3. Cartesian reference system and lengths for the UR10 robot.

The Denavit - Hartenberg (D-H) parameters of the Scara T6 and UR10 robots are shown in Table III and Table IV, respectively [22-24].

TABLE III. D-H PARAMETERS FOR SCARA T6 ROBOT

Joint	Scara T6 Robot			
	θ	d	a	α
1	θ_1	0	a_1	0
2	θ_2	0	a_2	0
3	0	$-\theta_3 - 0.083$	0	0

TABLE IV. D-H PARAMETERS FOR UR10 ROBOT

Joint	UR10 Robot			
	θ	d	a	α
1	q_1	L_1	0	$\pi/2$
2	q_2	0	L_2	0
3	q_3	0	L_3	0
4	q_4	L_4	0	$\pi/2$
5	q_5	L_5	0	$-\pi/2$
6	q_6	L_6	0	0

For the Scara T6 robot by multiplying all the transformation matrices in equation (2), the resulting matrix is:

$$T_3^0 = \begin{bmatrix} n_{3x} & o_{3x} & a_{3x} & P_{3x} \\ n_{3y} & o_{3y} & a_{3y} & P_{3y} \\ n_{3z} & o_{3z} & a_{3z} & P_{3z} \\ 0 & 0 & 0 & 1 \end{bmatrix} \quad (4)$$

Where the position of the end-effector is described by the position vector P_{3x1} (P_{3x}, P_{3y}, P_{3z}), then:

$$P_{3x} = a_2 C_{12} + a_1 C_1 \quad (5)$$

$$P_{3y} = a_2 S_{12} + a_1 S_1 \quad (6)$$

$$P_{3z} = -\theta_3 - 0.083 \quad (7)$$

The inverse kinematics for the Scara T6 robot was solved using the position vector P_{3x1} , obtaining:

$$\theta_1 = 2\text{atan}(t_1) \quad (8)$$

$$\theta_2 = \text{atan}\left(\pm\sqrt{1-t_2^2}/t_2\right) \quad (9)$$

$$\theta_3 = -P_{3z} \quad (10)$$

$$t_1 = \frac{-2P_{3y}a_1 \pm \sqrt{(2P_{3x}a_1)^2 + (2P_{3y}a_1)^2 - (a_2^2 - a_1^2 - P_{3x}^2 - P_{3y}^2)^2}}{a_2^2 - a_1^2 - P_{3x}^2 - P_{3y}^2 - 2P_{3x}a_1} \quad (11)$$

$$t_2 = \frac{P_{3x}^2 + P_{3y}^2 - a_1^2 - a_2^2}{2a_1a_2} \quad (12)$$

On the other hand, for Robot UR10 when multiplying the transformation matrices of equation (3), the resulting matrix is:

$$T_6^0 = \begin{bmatrix} n_{6x} & o_{6x} & a_{6x} & P_{6x} \\ n_{6y} & o_{6y} & a_{6y} & P_{6y} \\ n_{6z} & o_{6z} & a_{6z} & P_{6z} \\ 0 & 0 & 0 & 1 \end{bmatrix} \quad (13)$$

Where the position of the end effector is described by the vector (P_{6x}, P_{6y}, P_{6z}) , then:

$$P_{6x} = L_6(S_1 C_5 - C_1 C_{234} S_5) + L_4 S_1 + L_2 C_1 C_2 + L_5 C_1 S_{234} + L_3 C_1 (C_2 C_3 - S_2 S_3) \quad (14)$$

$$P_{6y} = L_2 S_1 C_2 - L_4 C_1 - L_6 (C_1 C_5 - S_1 C_{234} S_5) + L_5 S_1 S_{234} + L_3 S_1 (C_2 C_3 - S_2 S_3) \quad (15)$$

$$P_{6z} = L_1 + L_3 S_{23} + L_2 S_2 - L_5 C_{23} C_4 - S_{23} S_4 - L_6 S_5 (C_{23} S_4 + S_{23} C_4) \quad (16)$$

The inverse kinematics for the UR10 robot was solved using the iterative Gauss-Newton algorithm, which seeks to find the parameter values through an iterative multiplication of matrices [25, 26]. From the transformation matrix of Eq. (3), it follows that:

$$A_6^0 = T_6^0 \quad (17)$$

$$A_6^0 = A_1^0 A_2^1 A_3^2 A_4^3 A_5^4 A_6^5 \quad (18)$$

$$T_6^1(q_1, q_5, q_6) = (A_1^0)^{-1} T_6^0 \quad (19)$$

$$A_4^0 = A_1^0 A_2^1 A_3^2 A_4^3 \quad (20)$$

$$T_4^0(q_2, q_3, q_4) = T_6^0 (A_6^5)^{-1} (A_4^3)^{-1} \quad (21)$$

Then, the parameters are shown below:

$$q_1 = \text{atan2}(L_4, \text{sqrt}((P_{6x} - L_6 a_{6x})^2 + (L_6 a_{6y} - P_{6y})^2 - L_4^2)) - \text{atan2}(L_6 a_{6y} - P_{6y}, P_{6x} - L_6 a_{6x}) \quad (22)$$

$$q_2 = \text{atan2}(r_2, r_1) - \text{atan2}(L_3 S_3, L_2 + L_3 C_3) \quad (23)$$

$$q_3 = \text{atan2} \left(\sqrt{1 - \left(\frac{r_1^2 + r_2^2 - L_2^2 - L_3^2}{2L_2L_3} \right)^2}, \frac{r_1^2 + r_2^2 - L_2^2 - L_3^2}{2L_2L_3} \right) \quad (24)$$

$$q_4 = q_{234} - q_3 - q_2 \quad (25)$$

$$q_5 = \text{atan2} \left(\text{sqrt} \left((n_{6x}S_1 - n_{6y}C_1)^2 + (o_{6x}S_1 - o_{6y}C_1)^2 \right), a_{6x}S_1 - a_{6y}C_1 \right) \quad (26)$$

$$q_6 = \text{atan2} \left(\frac{-o_{6x}S_1 + o_{6y}C_1}{S_5}, \frac{n_{6x}S_1 - n_{6y}C_1}{S_5} \right) \quad (27)$$

$$q_{234} = \text{atan2}(n_{6z}C_5C_6 - a_{6z}S_5 - o_{6z}C_5S_6, o_{6z}C_6 + n_{6z}S_6) \quad (28)$$

$$r_1 = \text{sqrt} \left(\left(\text{sqrt} \left((P_{6x} - L_6a_{6x} + L_5o_{6x}C_6 + L_5n_{6x}S_6)^2 + (P_{6y} - L_6a_{6y} + L_5o_{6y}C_6 + L_5n_{6y}S_6)^2 \right) \right)^2 - L_4^2 \right) \quad (29)$$

$$r_2 = P_{6z} - L_6a_{6z} + L_5o_{6z}C_6 + L_5n_{6z}S_6 - L_1 \quad (30)$$

B. Dynamic Model

The dynamic model for the Scara T6 and UR10 robot was developed using the Newton - Euler formulation, analyzing the geometric relationships between each link, the position vector concerning the i -nth system (ri0pi), and the center of the mass vector of element i concerning its system (ri0si) [27,28].

Eq. (31) and (32) allowed obtaining forces and moments for each element $i = 1, 2, 3, \dots, n$.

$$f_i = F_i + f_{i+1} = m_i \bar{a}_i + f_{i+1} \quad (31)$$

$$n_i = n_{i+1} + \dot{p}_i x f_{i+1} + (\dot{p}_i + \bar{s}_i) x F_i + N_i \quad (32)$$

The physical parameters of each link such as length, mass, center of mass, and inertia tensor, were calculated using CAD modeling designed in SolidWorks, as shown in Fig. 4 and Fig.5 [29-31]. The following steps were followed to obtain it:

- 3D modeling of each element of the Scara T6 and UR10 robots using SolidWorks.
- Generate a separate solid model for each robot link, which should incorporate all significant features, including the motor, bearings, and any other components that contribute to the weight of the link.
- Assign the corresponding material to each component of the robots.
- Identify the primary coordinate system of each link, ensuring alignment with the Denavit - Hartenberg coordinate system. In the event of non-alignment, a new coordinate system should be introduced. Subsequently, upon accessing the properties section in SolidWorks, a summary of the physical property values is displayed, such as mass, center of mass (riosi), and moment of inertia of the link relative to the assigned output coordinate system.
- Finally, use the measurement tool in SolidWorks to draw lines and obtain the length value and the position

vector relative to the i -th coordinate system (riopi) of each link.

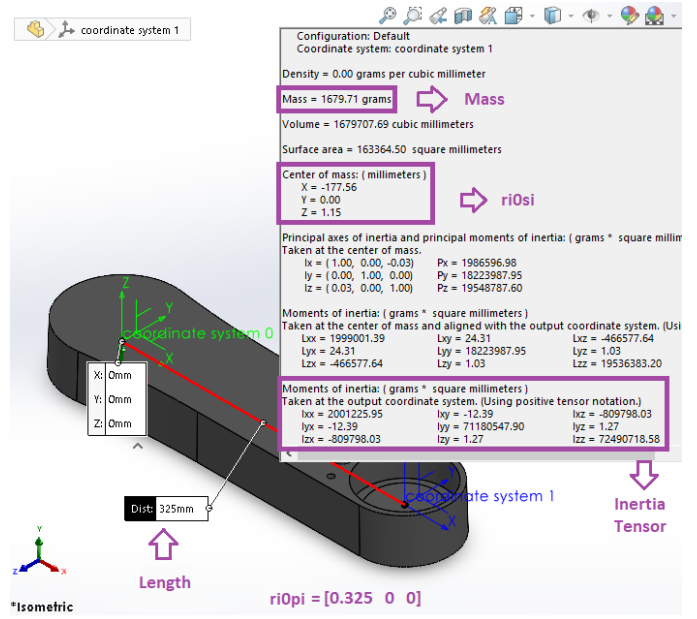


Fig. 4. Physical properties of scaraT6 robot link 1.

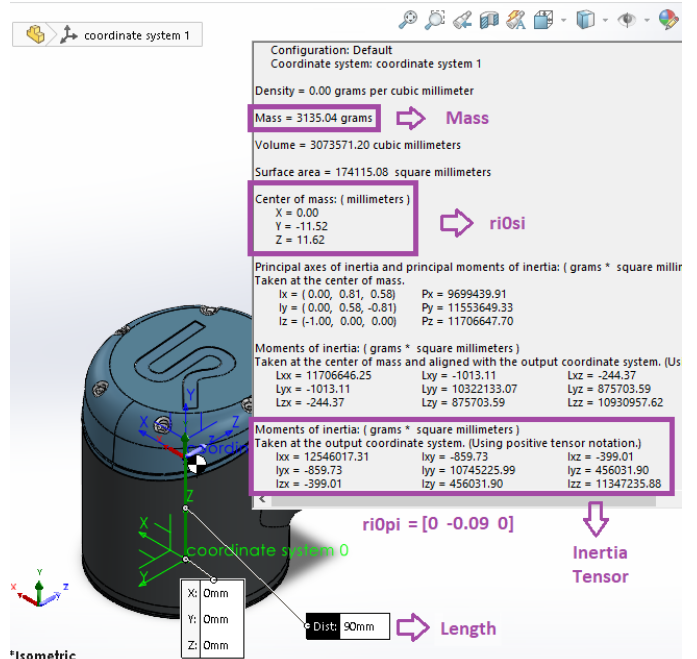


Fig. 5. Physical properties of UR10 robot link 1.

Then the torque for each joint is expressed in equation (33):

$$\tau_i = \begin{cases} n_i^T Z_{i-1} + b_i \dot{q}_i \\ f_i^T Z_{i-1} + b_i \dot{q}_i \end{cases} \quad (33)$$

Where b_i is the coefficient of viscous friction of each joint [32,33].

The parameters obtained from the links were used for the dynamic modeling of the Scara T6 and UR10 robots [34 and [35] which are shown in Table V and Table VI.

TABLE V. PARAMETERS FOR THE DYNAMICS OF THE SCARA T6 ROBOT

n	Scara T6 Robot				
	Length (mm)	Mass (kg)	Inertia Tensor (kgm ²)	riopi (m)	riosi (m)
1	325	1.68	$\begin{bmatrix} 0 & 0 & -0 \\ 0 & 0.07 & 0 \\ -0 & 0 & 0.07 \end{bmatrix}$	$\begin{bmatrix} 0.325 \\ 0 \\ 0 \end{bmatrix}$	$\begin{bmatrix} -0.18 \\ 0 \\ 0.001 \end{bmatrix}$
2	275	7.54	$\begin{bmatrix} 0.15 & 0 & -0.15 \\ 0 & 0.4 & 0 \\ -0.15 & 0 & 0.265 \end{bmatrix}$	$\begin{bmatrix} 0.275 \\ 0 \\ 0 \end{bmatrix}$	$\begin{bmatrix} -0.16 \\ 0 \\ 0.126 \end{bmatrix}$
3	-	0.08	$\begin{bmatrix} 0.006 & 0 & 0 \\ 0 & 0.006 & 0 \\ 0 & 0 & 0 \end{bmatrix}$	$\begin{bmatrix} 0 \\ 0 \\ -0.083 \end{bmatrix}$	$\begin{bmatrix} 0 \\ 0 \\ 0.246 \end{bmatrix}$

TABLE VI. PARAMETERS FOR THE DYNAMICS OF THE UR10 ROBOT

n	UR10 Robot				
	Length (mm)	Mass (kg)	Inertia Tensor (kgm ²)	riopi (m)	riosi (m)
1	90	3.14	$\begin{bmatrix} 0.013 & 0 & 0 \\ 0 & 0.01 & 0 \\ 0 & 0 & 0.01 \end{bmatrix}$	$\begin{bmatrix} 0 \\ 0.09 \\ 0 \end{bmatrix}$	$\begin{bmatrix} 0 \\ -0.0115 \\ 0.0116 \end{bmatrix}$
2	613	8.89	$\begin{bmatrix} 0.28 & 0 & -0.54 \\ 0 & 1.89 & 0 \\ -0.54 & 0 & 1.62 \end{bmatrix}$	$\begin{bmatrix} 0.613 \\ 0 \\ 0 \end{bmatrix}$	$\begin{bmatrix} -0.3618 \\ 0 \\ 0.17034 \end{bmatrix}$
3	572	4.75	$\begin{bmatrix} 0.02 & 0 & -0.08 \\ 0 & 0.69 & 0 \\ -0.08 & 0 & 1.63 \end{bmatrix}$	$\begin{bmatrix} 0.572 \\ 0 \\ 0 \end{bmatrix}$	$\begin{bmatrix} -0.3147 \\ 0 \\ 0.05142 \end{bmatrix}$
4	164	0.74	$\begin{bmatrix} 0.001 & 0 & 0 \\ 0 & 0.001 & 0 \\ 0 & 0 & 0.01 \end{bmatrix}$	$\begin{bmatrix} 0 \\ 0.164 \\ 0 \end{bmatrix}$	$\begin{bmatrix} 0 \\ -0.0076 \\ 0.00974 \end{bmatrix}$
5	116	0.74	$\begin{bmatrix} 0.001 & 0 & 0 \\ 0 & 0.001 & 0 \\ 0 & 0 & 0.01 \end{bmatrix}$	$\begin{bmatrix} 0 \\ -0.12 \\ 0 \end{bmatrix}$	$\begin{bmatrix} 0 \\ 0.0076 \\ 0.00974 \end{bmatrix}$
6	176	0.41	$\begin{bmatrix} 0.003 & 0 & 0 \\ 0 & 0.003 & 0 \\ 0 & 0 & 0.001 \end{bmatrix}$	$\begin{bmatrix} 0 \\ 0 \\ 0.176 \end{bmatrix}$	$\begin{bmatrix} 0 \\ 0.00477 \\ -0.0792 \end{bmatrix}$

From Eq. (31-33) considering b_i negligible and replacing the calculated parameters, the dynamic equations for the Scara T6 robot were obtained:

$$\tau_{1,3} = (1.294 + I_{ext} + 0.181m_{ext} + 0.601C_2 + 0.179m_{ext}C_2)qpp_1 + (0.38 + I_{ext} + 0.076m_{ext} + 0.301C_2 + 0.089m_{ext}C_2)qpp_2 - (0.301S_2 + 0.089m_{ext}S_2)qp_2^2 - (0.061S_2 + 0.179m_{ext}S_2)qp_1qp_2 \quad (34)$$

$$\tau_{2,3} = (0.38 + I_{ext} + 0.076m_{ext} + 0.301C_2 + 0.089m_{ext}C_2)qpp_1 + (0.38 + I_{ext} + 0.076m_{ext})qpp_2 + (0.301S_2 + 0.089m_{ext}S_2)qp_1^2 \quad (35)$$

$$\tau_{3,3} = (m_{ext} + 0.083)(qpp_3 + 9.81) \quad (36)$$

In the same way, the dynamic equations for the UR10 robot were obtained by solving Eq. (31), (32), and (33). By resolving

the dynamics of both robots, the Walker-Orin algorithm (inverse kinematics) is applied to validate the results and potentially facilitate dynamic control [36], [37].

C. Path Tracking Calculation

Kinematic control was performed using Matlab software to develop the desired movements according to the assigned tasks. The developed algorithm "planner" includes the starting and braking times of each motor, as well as the maximum speeds (rad/s) of each robot according to the manufacturer's data sheet [38, 39], for the planning of a smooth trajectory a 4-3-4 interpolator was implemented between the start and end point in the joint coordinates, returning the position, velocity, and acceleration matrices as a result [40-42].

Taking the initial and final points of the path taken by each robot (P_{nx1}), and considering their respective orientations ($R_{n \times n}$), the position, velocity, and acceleration graphs were obtained, as well as their trajectories in the 3D plane, which are shown in Fig. 6 to 9 [43-45].

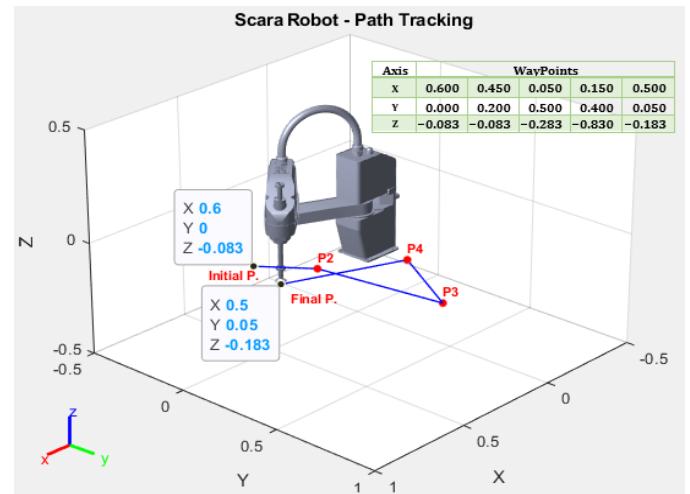


Fig. 6. Path tracking in matlab for scara T6 robot.

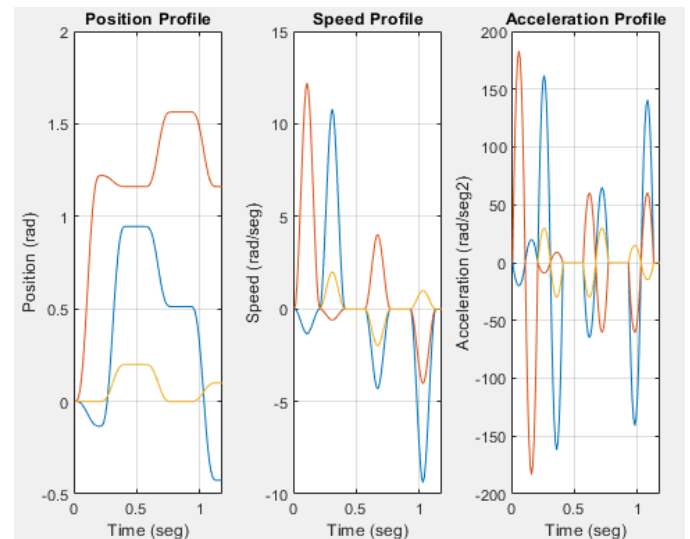


Fig. 7. Trajectory plot in matlab for scara T6 robot.

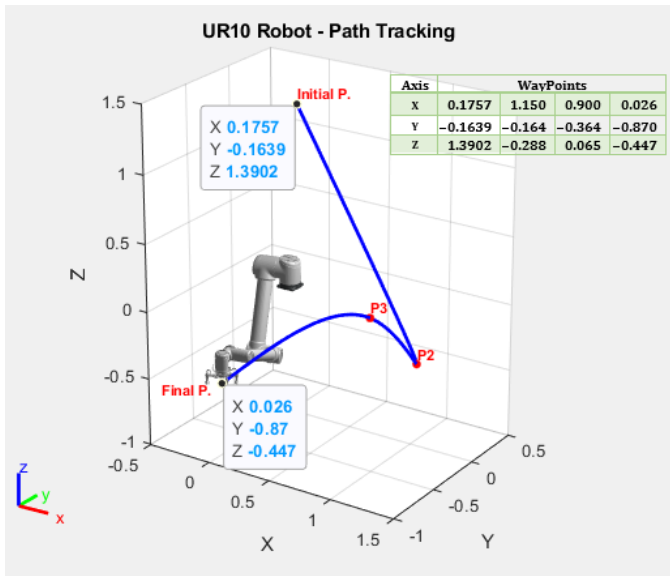


Fig. 8. Path tracking in matlab for UR10 robot.

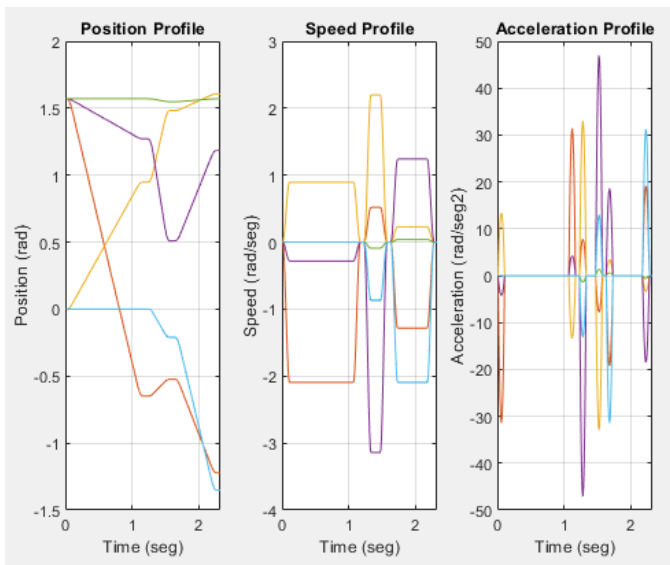


Fig. 9. Trajectory plot in matlab for UR10 robot.

D. Pick and Place and Palletizing Cell Simulation

The data of the joint positions obtained with the kinematic control were saved in matrices called "math_scara" and "math_ur10" respectively, to perform a real simulation in the CoppeliaSim environment [46], [47].

Facilities of the agro-exporting company Camposol were replicated using equipment such as crates, protective enclosures, smooth and roller conveyors provided by CoppeliaSim, along with those designed in SolidWorks, including the SCARA T6 and UR10 robots and the avocado [48], [49]

The designs generated in SolidWorks were then saved in URDF format, including their respective reference systems following the Denavit-Hartenberg method, to enable their visualization in the CoppeliaSim simulation environment to create a highly realistic virtual environment [50-52].

The SolidWorks URDF CAD files of the Scara T6 and UR10 robots were imported into CoppeliaSim, with the relevant parameters for real-time simulation, such as maximum torque (Nm) and maximum speed (°/s), being configured based on the manufacturer's datasheet. This process is illustrated in Fig. 10 [53-55].

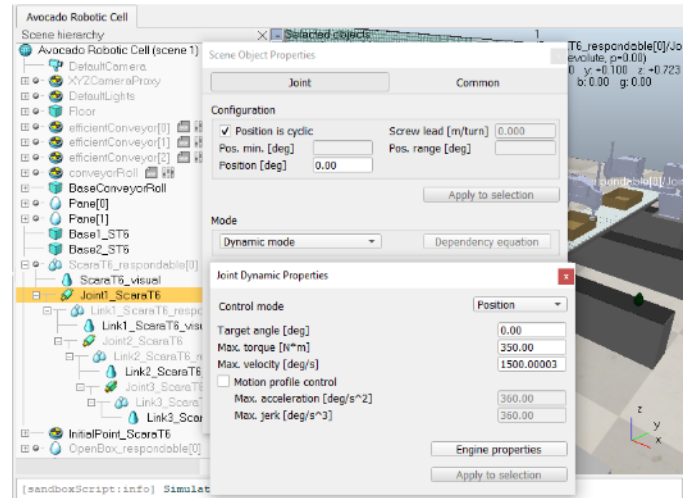


Fig. 10. Creation of the working environment and configuration of the Scara T6 y UR10 robots.

III. TESTS AND RESULTS

Fig.11 shows the Scara T6 robot picking up the avocado, starting from its resting position (a), and then placed in a cardboard box (b), at a maximum speed of 1500 °/s in its rotational joints and of 10 m/s in its prismatic joint, with a cycle time of 0.49 s. The task is performed until 20 Hass avocados of 22 – 24 calibers are placed in each box (c), then the suction cup type tool is activated, taking the box to the pallet to be grouped in three rows and three columns (d), at a maximum speed of 120 °/s for the base and shoulder joints, 180 °/s for the elbow and wrist, with a cycle time of 0.5 s. The task is executed up to palletizing 90 boxes.

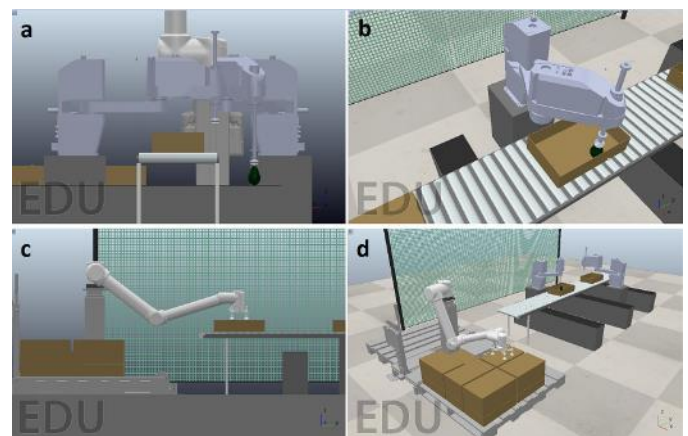


Fig. 11. Simulation in CoppeliaSim for scara T6 and UR10 robots.

The cell movements for pick and place and palletizing were simulated in CoppeliaSim. Table VII shows the working time of each path for both robots. A total working time of 1.18 s was obtained for the Scara T6 robot and 2.32 s for the UR10 robot.

For maximum range position $[\pi/2 \text{ rad/s}, \pi/2 \text{ rad/s}, 0.2 \text{ m}]$ for the Scara T6 robot and $[0, 0, 0, 0, 0, 0, 0]$ rad/s for the UR10, the maximum torques $[360.70, 146.30, 0.376]$ Nm and $[62.88, 116.20, 40.56, 9.25, 6.73, 4.34]$ Nm was obtained for each joint of both robots, as shown in Fig. 12.

TABLE VII. WORKING TIME IN EACH STATION

Path	Working Time	
	Scara T6 Robot (s)	UR10 Robot (s)
1 - 2	0.20	1.22
2 - 3	0.36	0.40
3 - 4	0.36	0.70
4 - 5	0.26	-
TOTAL	1.18	2.32

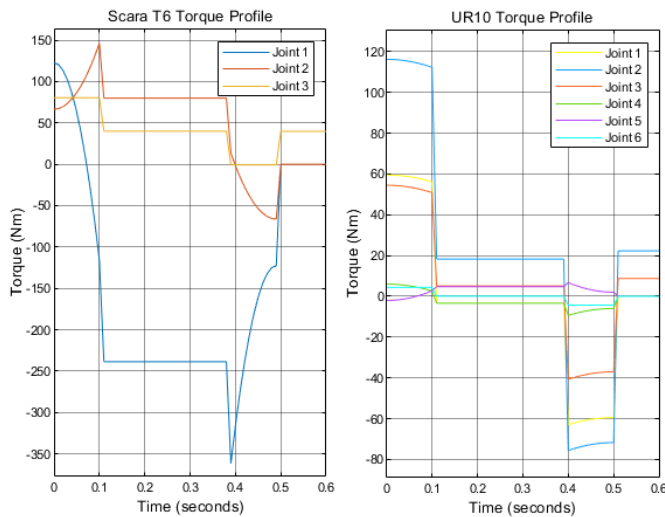


Fig. 12. Torque plot in simulink for scara T6 y UR10 robots.

IV. CONCLUSIONS AND FUTURE WORK

The mathematical models obtained using the Denavit-Hartenberg algorithm of the Scara T6 and UR10 robots were validated with the inverse kinematics tests developed in Matlab, and the models describing the inverse Newton Euler dynamics of the Scara T6 and UR10 robots were validated with the forward dynamics of Walker Orin developed in Matlab. With the "planner" algorithm developed, it was possible to follow the waypoints with smooth movements in each of the joints of the Scara T6 and UR10 robot, as evidenced in the graphs of the positioning, velocity, and acceleration profiles obtained. This significantly influences the accurate execution of pick and place as well as palletizing tasks assigned to the robots within the simulation environment.

The movements and constraints of the global simulation in CoppeliaSim allowed us to get efficient results for the serial work of the Scara T6 robot and the UR10 in the pick and place and palletizing cell with a cycle time of 3.5 s. According to the torque graphs obtained with Simulink, the maximum values for the Scara T6 robot and the UR10 robot showed a minimum difference of 3.06 % and 2.35 %, respectively, concerning the manufacturer's datasheet that was input in the dynamic

configurations of each joint in CoppeliaSim for each robot. This set of actions, in turn, leads to a significant reduction in the time required for the avocado packing process compared to human labor. This is especially relevant since more human personnel would be needed to achieve equivalent performance.

During 2023 – 2025, it is proposed to implement the pick and place tasks in a palletizing cell at the Camposol company located in the district of the Chao, La Libertad region, including a dynamic controller for both robots. In addition, this work not only complements previous research but also opens the door to the possibility of replicating this same application at an industrial level throughout South America and in countries that also produce and export avocados. This allows for the potential to export avocados on a large scale. Thus, meeting increased demand would no longer be an unattainable challenge.

REFERENCES

- [1] ComexPerú, "Las exportaciones de palta cayeron un 9.5% entre enero y agosto de este año," *ComexPerú*, 2022. <https://www.comexperu.org.pe/articulo/las-exportaciones-de-palta-cayeron-un-95-entre-enero-y-agosto-de-este-ano>
- [2] R. Gestión, "Las razones detrás de la caída de las exportaciones de palta peruana," *Redacción Gestión*, 2022. <https://gestion.pe/economia/las-razones-detras-de-la-caida-de-las-exportaciones-de-palta-peruana-comex-noticia/>
- [3] Blue Berries, "Ranking de las diez principales empresas agroexportadoras peruanas," *Blue Berries*, 2022. <https://blueberriesconsulting.com/ranking-de-las-diez-principales-empresas-agroexportadoras-peruanas>
- [4] Redagrícola, "Camposol compra 1,000 ha en Uruguay," *Redagrícola*, 2018. <https://www.redagricola.com/pe/camposol-compra-1000-ha-uruguay>
- [5] S. Rosales, "Camposol priorizará packing de palta el 2021 y a partir del 2022 continuará su expansión," *Redacción Gestión*, 2020. <https://gestion.pe/economia/empresas/camposol-el-proximo-ano-priorizaremos-packing-de-palta-y-desde-2022-continuaremos-con-expansion-agroexportaciones-noticia/>
- [6] T. Dewi, P. Risma, and Y. Oktarina, "Fruit sorting robot based on color and size for an agricultural product packaging system," *Bulletin of Electrical Engineering and Informatics*, vol. 9, no. 4, pp. 1438–1445, 2020, doi: 10.11591/eei.v9i4.2353.
- [7] X. Chen, Y. Zhou, B. Yang, X. Miao, Y. Li, and M. Zhang, "Designing Control System of Palletizing Robot Based on RobotStudio," *Journal of Physics: Conference Series*, vol. 2402, no. 1, 2022, doi: 10.1088/1742-6596/2402/1/012039.
- [8] M. Almaged, "Forward and Inverse Kinematic Analysis and Validation of the ABB IRB 140 Industrial Robot," *International Journal of Electronics, Mechanical and Mechatronics Engineering*, vol. 7, no. 2, pp. 1383–1401, 2017, doi: 10.17932/iau.ijemme.21460604.2017.7/2.1383-1401.
- [9] B. Tipary and G. Erdős, "Generic development methodology for flexible robotic pick-and-place workcells based on Digital Twin," *Robotics and Computer-Integrated Manufacturing*, vol. 71, 2021, doi: 10.1016/j.rcim.2021.102140.
- [10] M. Agarwal, S. Biswas, C. Sarkar, S. Paul, and H. S. Paul, "Jampacker: An Efficient and Reliable Robotic Bin Packing System for Cuboid Objects," *IEEE Robotics and Automation Letters*, vol. 6, no. 2, pp. 319–326, 2021, doi: 10.1109/LRA.2020.3043168.
- [11] O. J. V. Ramirez, J. E. Cruz De La Cruz, W. A. M. MacHaca, "Agroindustrial Plant for the Classification of Hass Avocados in Real-Time with ResNet-18 Architecture," *2021 5th International Conference on Robotics and Automation Sciences, ICRAS 2021*, pp. 206–210, 2021, doi: 10.1109/ICRAS52289.2021.9476659.
- [12] J. P. Vásquez, F. A. Auat Cheein, "Workload and production assessment in the avocado harvesting process using human-robot

- collaborative strategies,” *Biosystems Engineering*, vol. 223, pp. 56–77, 2022, doi: 10.1016/j.biosystemseng.2022.08.010.
- [13] X. Liu, Y. Zhao, D. Geng, S. Chen, X. Tan, C. Cao, “Soft Humanoid Hands with Large Grasping Force Enabled by Flexible Hybrid Pneumatic Actuators,” *Soft Robotics*, vol. 8, no. 2, pp. 175–185, 2021, doi: 10.1089/soro.2020.0001.
- [14] UNITED NATIONS, “Sustainable Development Goals,” *UNITED NATIONS*, 2023. <https://www.un.org/sustainabledevelopment/>
- [15] Aguacate Hass y Méndez, “Tabla de calibres aguacate de exportación,” *simpaq*, 2022. <https://www.simpaq.mx/producto>
- [16] Unifrutti, “Embalaje / paletizaje,” *unifrutti*, 2022. <https://www.unifrutti.com/productos/paltas/embalaje-paletizaje/>
- [17] J. Huanca, J. Zamora, J. Cornejo, and R. Palomares, “Mechatronic Design and Kinematic Analysis of 8 DOF Serial Robot Manipulator to Perform Electrostatic Spray Painting Process on Electrical Panels,” *Proceedings of the 2022 IEEE Engineering International Research Conference, EIRCON 2022*, 2022, doi: 10.1109/EIRCON56026.2022.9934104.
- [18] J. Cornejo, J. Palacios, A. Escobar, and Y. Torres, “Mechatronics Design and Kinematic Simulation of UTP-ISR01 Robot with 6-DOF Anthropomorphic Configuration for Flexible Wall Painting,” *2022 1st International Conference on Electrical, Electronics, Information and Communication Technologies, ICEEICT 2022*, 2022, doi: 10.1109/ICEEICT53079.2022.9768599.
- [19] D. He, F. Liu, and F. Wang, “Optimal Design of Industrial Robot Kinematics Algorithm,” *Journal of Physics: Conference Series*, vol. 1624, no. 4, pp. 3–7, 2020, doi: 10.1088/1742-6596/1624/4/042029.
- [20] S. Kana, J. Gurnani, V. Ramanathan, S. H. Turlapati, M. Z. Ariffin, and D. Campolo, “Fast Kinematic Re-Calibration for Industrial Robot Arms,” *Sensors*, vol. 22, no. 6, 2022, doi: 10.3390/s22062295.
- [21] G. Gao, G. Sun, J. Na, Y. Guo, and X. Wu, “Structural parameter identification for 6 DOF industrial robots,” *Mechanical Systems and Signal Processing*, vol. 113, pp. 145–155, 2018, doi: 10.1016/j.ymsp.2017.08.011.
- [22] H. Chen, N. Zhou, and R. Wang, “Design and Dimensional Optimization of a Controllable Metamorphic Palletizing Robot,” *IEEE Access*, vol. 8, pp. 123061–123074, 2020, doi: 10.1109/ACCESS.2020.3007707.
- [23] O. J. V. Ramirez, J. E. Cruz De La Cruz, and W. A. M. MacHaca, “Agroindustrial Plant for the Classification of Hass Avocados in Real-Time with ResNet-18 Architecture,” *2021 5th International Conference on Robotics and Automation Sciences, ICRAS 2021*, pp. 206–210, Jun. 2021, doi: 10.1109/ICRAS52289.2021.9476659.
- [24] J. Cornejo, V. Cruz, F. Carrillo, R. Cerda, and E. R. Sanchez Penadillo, “Mechatronics Design and Kinematic Simulation of SCARA Robot to improve Safety and Time Processing of Covid-19 Rapid Test,” *2022 1st International Conference on Electrical, Electronics, Information and Communication Technologies, ICEEICT 2022*, 2022, doi: 10.1109/ICEEICT53079.2022.9768506.
- [25] O. Mejia, D. Nunez, J. Razuri, J. Cornejo, and R. Palomares, “Mechatronics Design and Kinematic Simulation of 5 DOF Serial Robot Manipulator for Soldering THT Electronic Components in Printed Circuit Boards,” *2022 1st International Conference on Electrical, Electronics, Information and Communication Technologies, ICEEICT 2022*, 2022, doi: 10.1109/ICEEICT53079.2022.9768447.
- [26] J. Cornejo, R. Palomares, M. Hernandez, D. Magallanes, and S. Gutierrez, “Mechatronics Design and Kinematic Simulation of a Tripterion Cartesian-Parallel Agricultural Robot Mounted on 4-Wheeled Mobile Platform to Perform Seed Sowing Activity,” *2022 1st International Conference on Electrical, Electronics, Information and Communication Technologies, ICEEICT 2022*, 2022, doi: 10.1109/ICEEICT53079.2022.9768422.
- [27] E. Re and A. Todas, “Robot Epson SCARA T6 All-in-One.” pp. 21–23.
- [28] U. Robots, “UR10e Technical Specifications.” p. 177.
- [29] M. A. González-Palacios, M. A. Garcia-Murillo, and M. González-Dávila, “A novel tool to optimize the performance of SCARA robots used in pick and place operations,” *Journal of Mechanical Science and Technology*, vol. 35, no. 10, pp. 4715–4726, Oct. 2021, doi: 10.1007/S12206-021-0937-X.
- [30] H. Chanal *et al.*, “Geometrical defect identification of a SCARA robot from a vector modeling of kinematic joints invariants,” *Mechanism and Machine Theory*, vol. 162, p. 104339, 2021, doi: 10.1016/j.mechmachtheory.2021.104339.
- [31] M. Ulrich and C. Steger, “Hand-eye calibration of SCARA robots using dual quaternions,” *Pattern Recognition and Image Analysis*, vol. 26, no. 1, pp. 231–239, 2016, doi: 10.1134/S1054661816010272.
- [32] H. Chih-Ching, K. Chin-Hsing, M. Daisuke, and T. Yukio, *Advances in Mechanism and Machine Science*, vol. 73, no. 16. Springer International Publishing, 2019. doi: 10.1007/978-3-030-20131-9.
- [33] P. K. Jamwal, A. Kapsalyamov, S. Hussain, and M. H. Ghayesh, “Performance based design optimization of an intrinsically compliant 6-dof parallel robot,” *Mechanics Based Design of Structures and Machines*, vol. 50, no. 4, pp. 1237–1252, 2022, doi: 10.1080/15397734.2020.1746669.
- [34] P. Li, T. Shu, W. F. Xie, and W. Tian, “Dynamic Visual Servoing of A 6-RSS Parallel Robot Based on Optical CMM,” *Journal of Intelligent and Robotic Systems: Theory and Applications*, vol. 102, no. 2, 2021, doi: 10.1007/s10846-021-01402-5.
- [35] M. Zhang and J. Yan, “A data-driven method for optimizing the energy consumption of industrial robots,” *Journal of Cleaner Production*, vol. 285, p. 124862, 2021, doi: 10.1016/j.jclepro.2020.124862.
- [36] L. F. F. Furtado, E. Villani, L. G. Trabasso, and R. Sutério, “A method to improve the use of 6-dof robots as machine tools,” *International Journal of Advanced Manufacturing Technology*, vol. 92, no. 5–8, pp. 2487–2502, 2017, doi: 10.1007/s00170-017-0336-8.
- [37] P. Bobka, F. Gabriel, and K. Dröder, “Fast and precise pick and place stacking of limp fuel cell components supported by artificial neural networks,” *CIRP Annals*, vol. 69, no. 1, pp. 1–4, 2020, doi: 10.1016/j.cirp.2020.04.103.
- [38] Ş. Yıldırım and S. Savaş, “Design of a Mobile Robot to Work in Hospitals and Trajectory Planning Using Proposed Neural Networks Predictors,” *Lecture Notes in Networks and Systems*, vol. 305, no. 9, pp. 32–45, 2022, doi: 10.1007/978-3-030-83368-8_4.
- [39] B. Belzile, P. K. Eskandary, and J. Angeles, “Workspace Determination and Feedback Control of a Pick-And-Place Parallel Robot: Analysis and Experiments,” *IEEE Robotics and Automation Letters*, vol. 5, no. 1, pp. 40–47, 2020, doi: 10.1109/LRA.2019.2945468.
- [40] Z. A. Karam and E. A. Saeed, “Smartly Control, Interface and Tracking for Pick and Place Robot Based on Multi Sensors and Vision Detection,” *International Journal of Computing and Digital Systems*, vol. 12, no. 1, pp. 1215–1229, 2022, doi: 10.12785/ijcds/120197.
- [41] D. Ionescu *et al.*, “Communication and Control of an Assembly, Disassembly and Repair Flexible Manufacturing Technology on a Mechatronics Line Assisted by an Autonomous Robotic System,” *Inventions*, vol. 7, no. 2, 2022, doi: 10.3390/inventions7020043.
- [42] S. Li, D. Chen, and J. Wang, “A TRAJECTORY TRACKING METHOD OF PARALLEL MANIPULATOR BASED ON KINEMATIC CONTROL ALGORITHM,” *International Journal of Robotics and Automation*, vol. 37, no. 3, pp. 273–279, 2022, doi: 10.2316/J.2022.206-0577.
- [43] A. Singletary, S. Kolathaya, and A. D. Ames, “Safety-Critical Kinematic Control of Robotic Systems,” *IEEE Control Systems Letters*, vol. 6, no. c, pp. 139–144, 2022, doi: 10.1109/LCSYS.2021.3050609.
- [44] P. Boscaroli and D. Richiedei, “Trajectory design for energy savings in redundant robotic cells,” *Robotics*, vol. 8, no. 1, 2019, doi: 10.3390/robotics8010015.
- [45] Q. Xiao, G. Xiang, Y. Chen, Y. Zhu, and S. Dian, “Time-Optimal Trajectory Planning of Flexible Manipulator Moving along Multi-Constraint Continuous Path and Avoiding Obstacles,” *Processes*, vol. 11, no. 1, 2023, doi: 10.3390/pr11010254.
- [46] T. P. Kapusi, T. I. Erdei, G. Husi, and A. Hajdu, “Application of Deep Learning in the Deployment of an Industrial SCARA Machine for Real-Time Object Detection,” *Robotics*, vol. 11, no. 4, 2022, doi: 10.3390/robotics11040069.
- [47] R. Chiba, T. Arai, T. Ueyama, T. Ogata, and J. Ota, “Working environment design for effective palletizing with a 6-DOF manipulator,” *International Journal of Advanced Robotic Systems*, vol. 13, no. 2, pp. 1–8, 2016, doi: 10.5772/62345.

- [48] D. A. Jimenez-Nixon, M. C. Paredes-Sanchez, and A. M. Reyes-Duke, "Design, construction and control of a SCARA robot prototype with 5 DOF," *Proceedings of the 2022 IEEE International Conference on Machine Learning and Applied Network Technologies, ICMLANT 2022*, 2022, doi: 10.1109/ICMLANT56191.2022.9996479.
- [49] M. E. Uk, F. B. Sajjad Ali Shah, M. Soyaslan, and O. Eldogan, "Modeling, control, and simulation of a SCARA PRR-type robot manipulator," *Scientia Iranica*, vol. 27, no. 1, pp. 330–340, 2020, doi: 10.24200/sci.2018.51214.2065.
- [50] A. Bahani, M. E. houssine Ech-Chhibat, H. Samri, and H. A. Elattar, "The Inverse Kinematics Evaluation of 6-DOF Robots in Cooperative Tasks Using Virtual Modeling Design and Artificial Intelligence Tools," *International Journal of Mechanical Engineering and Robotics Research*, pp. 121–130, 2023, doi: 10.18178/IJMERR.12.2.121-130.
- [51] H. Zhu, W. Xu, B. Yu, F. Ding, L. Cheng, and J. Huang, "A Novel Hybrid Algorithm for the Forward Kinematics Problem of 6 DOF Based on Neural Networks," *Sensors*, vol. 22, no. 14, pp. 1–18, 2022, doi: 10.3390/s22145318.
- [52] A. Córdova, P. Quimbiamba, L. J. Segura, L. Escobar, and D. Loza, "Implementation of Collaborative Work Between Two SCARA Robots in a Robotic Cell for Continuous Classification of Products," *Lecture Notes in Electrical Engineering*, vol. 932 LNEE, pp. 97–111, 2022, doi: 10.1007/978-3-031-08288-7_7.
- [53] C. Han, H. Ma, W. Zuo, S. Chen, and X. Zhang, "A general 6-DOF industrial robot arm control system based on Linux and FPGA," *Proceedings of the 30th Chinese Control and Decision Conference, CCDC 2018*, pp. 1220–1225, 2018, doi: 10.1109/CCDC.2018.8407315.
- [54] P. Ji, C. Li, and F. Ma, "Sliding Mode Control of Manipulator Based on Improved Reaching Law and Sliding Surface," *Mathematics*, vol. 10, no. 11, 2022, doi: 10.3390/math10111935.
- [55] J. Cornejo *et al.*, "Industrial, Collaborative and Mobile Robotics in Latin America: Review of Mechatronic Technologies for Advanced Automation," *Emerging Science Journal*, 2023.